DOI: 10.61782/fa.2025.0578

MODELLING CROSS-LAMINATED TIMBER PLATE CONNECTIONS: A NUMERICAL INVESTIGATION ON FLANKING SOUND TRANSMISSION THROUGH ANGLE BRACKETS

Antonio Esposito[1*] **Sven Vallely**[1,2] **Stefan Schoenwald**[1]

[1] Laboratory for Acoustics/Noise Control, Empa, Switzerland
[2] Department of Civil Engineering – Structural Mechanics Section, KU Leuven, Belgium

ABSTRACT

In recent years, interest has grown in numerical models to predict flanking sound transmission through Cross-Laminated Timber (CLT) junctions. The panels are typically connected with screwed metal brackets, which are differently shaped depending on the junction geometry and structural requirements. To predict the Vibration Reduction Index K_{ij}, available models rely either on empirical formulae or simplified junctions with idealized connection. In this contribution, a numerical investigation on the dynamics of a CLT L-junction is presented, starting from a detailed representation of an angle bracket. This was modelled in FEM and validated with vibrometry measurements. It was then integrated into the model of a CLT L-junction mock-up and compared to experimental datasets from two different configurations, where CLT plates were either in direct contact or separated by an air gap. Validation in the modal domain showed a good agreement of the model with both experimental configurations. The comparison with experimental K_{ij} showed a better correlation with the latter configuration, whereas larger deviations were observed above 1 kHz in the former case. This provided some insights on the modelling of bracket fastening and highlighted the need of introducing constraint conditions at the interface between CLT plates to simulate the effects of direct contact.

**Corresponding author*: *antonio.esposito@empa.ch.*

Keywords: *Cross-Laminated Timber, Flanking Sound Transmission, Vibration Reduction Index, Finite Element Method.*

1. INTRODUCTION

The use of Cross-Laminated Timber (CLT) has become well established in the construction industry due to its proven benefits in terms of structural efficiency, cost-effectiveness and environmental sustainability. CLT plates are often employed as load-bearing elements, due to their orthotropy and high strength-to-weight ratio. On the other hand, this feature causes significant structure-borne sound power flow across their junctions [1]. CLT plates are usually connected with screwed metal brackets, especially for specific types like L-, T- or X- junctions [2]. Given the above, the numerical modelling of flanking vibration transmission mechanisms in CLT junctions has received particular attention, with the aim of predicting the Vibration Reduction Index K_{ij}, as defined in the ISO 12354-1:2017 [3] and the ISO 10848-1:2017 [4] standards. The computation of this quantity becomes critical since the interface between CLT plates is, in most cases, both punctual, due to fasteners, and linear, due to the contact between plates [2]. Existing predictive approaches rely either on empirical or analytical models. In particular, the ISO 12354:2017-1 standard [3] provides empirical formulae, based on laboratory measurements, to compute K_{ij} for T- and X- CLT junctions. Nevertheless, such relationships are considered valid only within a limited range of area mass density ratios between the elements. In addition to empirical models, various analytical or numerical approaches for modelling CLT junctions can be found in the literature. Among others, Salvalaggio et al. [5] investigated the impact of sound-insulated joints on the dynamics of CLT structures. In their study, plate joints with steel fasteners were modelled as linear interface elements and angle brackets as nodal linear springs, whose stiffnesses were retrieved from a model updating process. In a recent work, Moons et al. [6] proposed an efficient analytical wave approach to predict K_{ij} through CLT junctions with and without resilient interlayers. Their model without interlayers showed deviations against experiments below 5 dB in 1/3 octave bands up to 2000 Hz. In this latter case, CLT plates were modeled as semi-infinite, assuming ideal rigid connections. In the context of the research project "Schallschutz im Holzbau", conducted in a cooperation between Lignum (Swiss Forestry Association) and Empa, the dynamic behavior of metal angle brackets was analyzed with the aim of investigating the effects of point connections between plates on CLT junctions. A steel angle bracket has been modelled in FEM and validated with laser doppler vibrometry measurements in the modal domain. It has been then integrated in a global FEM model of a CLT L-junction mock-up. The numerical K_{ij} was computed and compared against the experimental K_{ij} obtained by measuring two different setups, in which plates, connected with two angle brackets, were either in direct contact or separated by a 3 mm air gap. Based on the above, an alternative approach is proposed herein, for the dynamic characterization of CLT junction components. This may constitute a preliminary stage of a bottom-up procedure for setting up broadband versatile FEM models, which could possibly account for the effects of a change in the number and position of connectors in the junction. Please note that the graphs presented in this updated version of the paper are revised with respect to that initially submitted for the conference.

2. THEORY AND BACKGROUND

In the following subsections, the basic principles of FEM modal and harmonic analyses, conducted on the proposed models, are outlined. Furthermore, the theoretical background underlying the Vibration Reduction Index K_{ij} is summarized, since it was calculated and referred to as a validation of the numerical model of the L-junction.

2.1 Modal analysis

For an undamped multi-degree of freedom system, the equation of motion for free vibration is written as [7]:

$$[\mathbf{M}]\{\ddot{\mathbf{x}}\} + [\mathbf{K}]\{\mathbf{x}\} = 0 \tag{1}$$

where $\{\ddot{\mathbf{x}}\}$ is the nodal acceleration vector, $\{\mathbf{x}\}$ is the nodal displacement vector, $[\mathbf{M}]$ is the mass matrix and $[\mathbf{K}]$ is the stiffness matrix of the system. Assuming the displacement field solution of Eqn. (1) to be harmonic, the natural frequencies and the eigenvectors of the system can be calculated by solving the corresponding eigenvalue problem.

2.2 Harmonic analysis

When a damped system is excited by an external harmonic force $\{\mathbf{F}\}$, Eqn. (1) becomes [7]:

$$[\mathbf{M}]\{\ddot{\mathbf{x}}\} + [\mathbf{C}]\{\dot{\mathbf{x}}\} + [\mathbf{K}]\{\mathbf{x}\} = \{\mathbf{F}\} \tag{2}$$

where $\{\mathbf{F}\}$ is the external harmonic forcing vector and $[\mathbf{C}]$ is the structural damping matrix of the system.

2.3 Vibration Reduction Index K_{ij}

In order to predict the flanking sound transmission across a junction between building elements, the ISO 12354-1:2017 standard [3] introduces the Vibration Reduction Index K_{ij}. This quantity represents, analogously to the Sound Reduction Index, the attenuation of structure-borne sound at a junction. It is based on Statistical Energy Analysis simplifications on power transmission. It is frequency-dependent, expressed in decibels and defined as:

$$K_{ij} = \overline{Dv_{,ij}} + 10lg\left(\frac{l_{ij}}{\sqrt{a_i a_j}}\right). \tag{3}$$

where $\overline{Dv_{,ij}}$ is the direction-averaged velocity level difference between two elements, l_{ij} is the junction length and $a_{i,j}$ are the equivalent absorption lengths of the elements i and j. These are defined as [4]:

$$a = \frac{2.2\pi^2 S}{c_0 T_s}\sqrt{\frac{f_{ref}}{f}} \tag{4}$$

where T_s is the structural reverberation time of the element, S is the surface area of the element, f is the centre band frequency, f_{ref}, equal to 1000 Hz, is the reference frequency and c_0 is the speed of sound in air.

3. NUMERICAL MODELLING AND VALIDATION OF A STEEL ANGLE BRACKET

In the following subsections, the FEM model of a single steel angle bracket is described. The numerical and experimental setups are described and the validation of the FEM model in the modal domain is presented.

3.1 FEM model setup

An angle bracket was numerically modelled in Ansys Mechanical (Release 2024, R2) and its geometry was reproduced starting from that of a commercially available galvanized steel bracket (Fig. 1). The bracket is modelled as an elastic isotropic shell element and discretised by using 2 mm quadratic triangular mesh elements (Fig. 1), with a total number of 90546 degrees of freedom (DOFs). Elasticity parameters for DX51D galvanized steel are drawn from [8] and listed in Tab. 1.

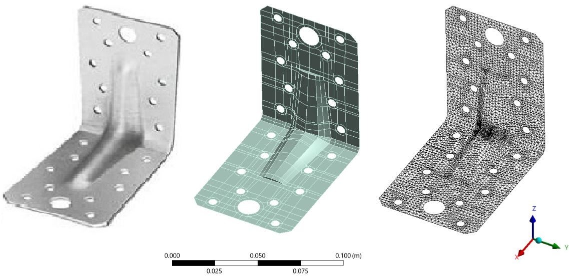

Figure 1. Left-hand side: commercial sample of the analyzed galvanized steel angle bracket. Center: CAD geometry of the bracket sample. Right-hand side: meshed geometry with 2 mm quadratic triangular elements.

Table 1. Elastic constants of DX51D galvanized steel [8].

Mass density, ρ [kgm^{-3}]	Elastic modulus, E [GPa]	Poisson's ratio, ν [-]
7830	210	0.30

A FE modal analysis is performed on the bracket, which is assumed to be in free boundary conditions. Numerical results in terms of eigenfrequencies and modeshapes are reported in the subsection 3.2 and compared to experimental data for validation in the modal domain.

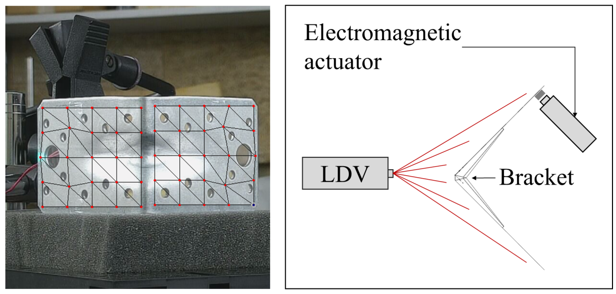

Figure 2. Setup of the experiment on a steel angle bracket. Left-hand side: laser vibrometer measurement grid. Right-hand side: schematic of the measurement setup.

3.2 Vibration measurements and validation in the modal domain

Vibration measurements on the steel angle bracket were carried out with a Laser Doppler Vibrometer. In order to ensure repeatability of the results, tests were performed on three different samples of the same bracket model. To replicate the free boundary conditions during measurements, brackets were resting on a layer of melamine foam. As visible in Fig. 2, they were excited at a corner position with an electromagnetic actuator to minimize possible alterations on mass and stiffness due to the use of a mechanical shaker. A grid of measurement points was set over the surface of the bracket to measure surface velocities (Fig. 2). Where possible, most of the points were evenly spaced on a 13 mm modular grid. The frequency range was from 0 Hz to 6.4 kHz with a spectral resolution of 500 mHz. Ten measurements were averaged at each point and point mobility was exported for each sample. As visible in Fig. 3a, the frequency response functions measured at a corner point were compared. The natural frequencies of the bracket were identified by the peaks of the mobility functions. At the corresponding frequencies, the measured modeshapes showed a good agreement with the numerical results (Fig. 3b and Fig. 3c). Furthermore, the percentage error between numerical and experimental eigenfrequencies was consistently below 5%, except for one eigenmode occurring at 3395.2 Hz, showing a 5.3% error against experimental data. Given the above, the FEM model of the steel angle bracket was considered validated.

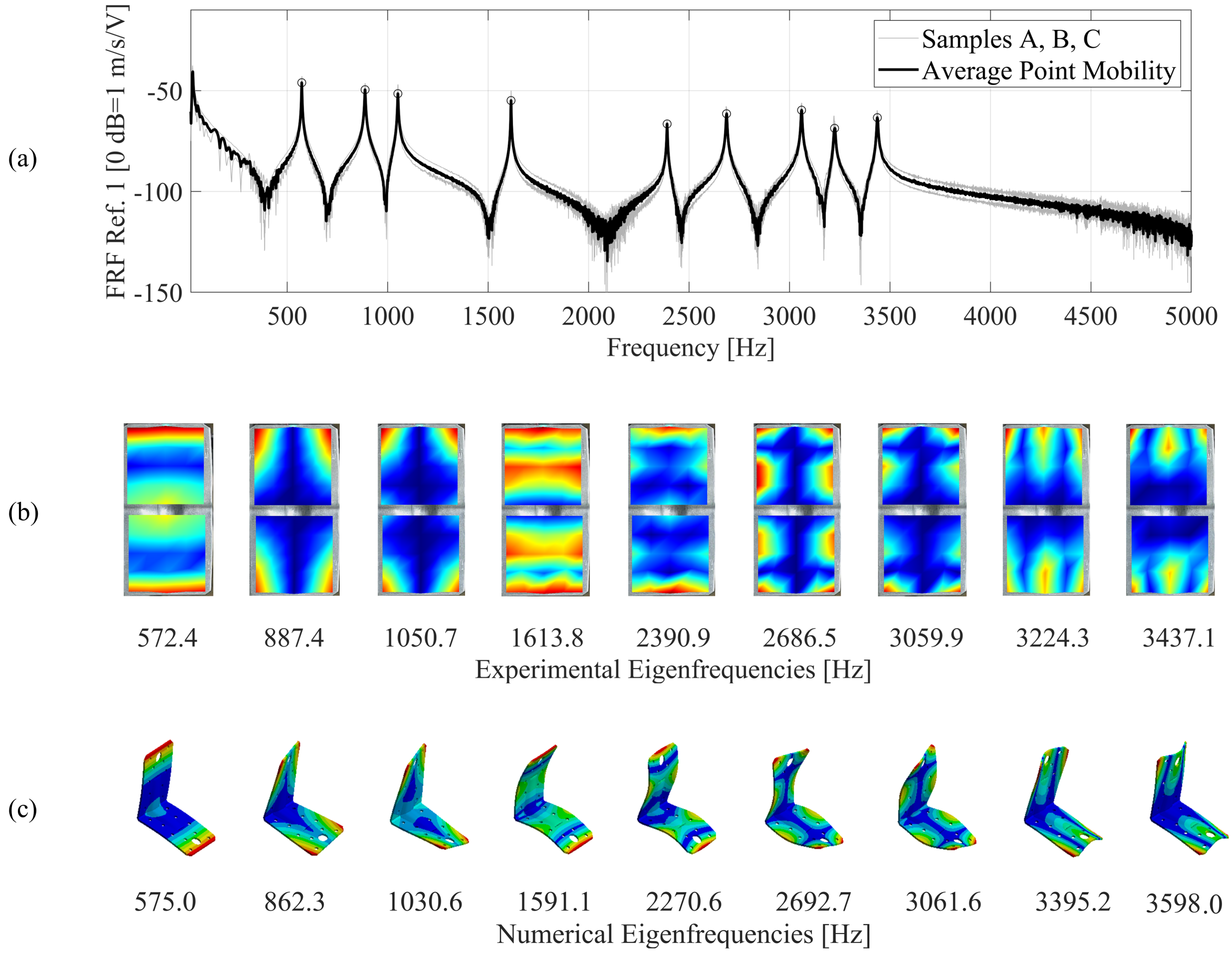

Figure 3. (a) Point Mobility response functions measured on three samples of the same angle bracket model (in gray). The average mobility is represented in black. Abscissas of circled peaks identify the eigenfrequencies of the bracket. (b) Measured modeshapes of the bracket and corresponding eigenfrequencies. (c) FEM modeshapes of the bracket and corresponding eigenfrequencies.

4. NUMERICAL MODELLING OF AN L-JUNCTION MOCK-UP

Once validated against experimental data, the FE model of the bracket was integrated into the numerical model of a CLT L-junction mock up. The latter was validated against laser vibrometry measurements in the modal domain. In the following subsections, the numerical model is described and the setup from two different experimental configurations is reported.

4.1 FEM model setup

A mock-up of a CLT L-junction has been modelled in FEM. Two CLT plates (henceforth referred to as CLT100A1 and CLT060C1) were connected along their short edge with two steel angle brackets (Fig. 4). Brackets were modelled as isotropic shells and meshed according to what mentioned in subsection 3.1. CLT plates were represented as two-dimensional orthotropic shells where the [90/0/90] orientation of the plies was implicitly modelled in a layer-wise representation. The plates were discretised using 4 cm quadratic triangular mesh elements (Fig. 4b). Physical connections at bracket-plate interface required a specific modelling approach. Multi Point Constraint (MPC) rigid joints were defined to tie nodal displacements at the edges of the bracket screw holes to the nodes defined on the adjacent plates, lying in correspondence of the hole edges projected from the bracket onto the plate surface. With MPC formulation, individual degrees of freedom defined along these edges were eliminated and forced to have the same solution as a single node placed at the origin of the joint reference system (Fig. 4c). Along the contact edge between the two plates, no constraint condition was introduced. Geometrical and mechanical properties of the plates are reported in Tab. 2. Elastic orthotropic parameters of CLT plates were obtained using a numerical parameter estimation based on vibration measurements conducted on the same plates individually. From the same set of measurements, frequency independent structural loss factors were obtained by applying the Power Injection Method (PIM) [1]. The description of the aformentioned procedures is based on the methods applied in [9] for material property derivation. Modal and full harmonic structural dynamic analyses were conducted for the L-junction system. In the former case, eigenfrequencies and modeshapes of the first fifteen modes were used for calculation of the Percentage Error (PE) and Modal Assurance Criterion (MAC) against experimental data for validation in the modal domain. The PE index provides the relative difference between numerical and experimental eigenfrequencies, expressed in percentage. The MAC index is defined as a squared linear regression correlation coefficient (ranging from 0 to 1) between numerical and experimental eigenvectors. The plates were excited by a transverse harmonic force at three different nodal positions for each plate, as depicted in Fig. 4a. The force amplitude was set as 1 N. The normal surface velocities were acquired as a function of frequency. The surface velocity response of the nodes were then mapped using two-dimensional linear interpolation to the grid measurement points used for the measurements with a laser vibrometer, as described in subsection 4.2. A logarithmic solution interval was defined for the full harmonic analysis, ranging from 200 Hz to 3150 Hz with 575 frequency steps.

4.2 Experimental setup

The numerical setup described in subsection 4.1 was replicated experimentally in the lightweight facility at Empa (Fig. 5a). CLT100A1 and CLT060C1 plates were connected with two steel angle brackets, each of which was fixed with four wood screws to the plates (Fig. 5a). In order to isolate the dynamic effects of bracket fastening onto CLT plates in the junction, two different configurations were setup: in the first, plates were touching each other along the common edge (configuration A in Fig. 5b); in the second, a 3 mm air gap was left between the plates, in order to ensure structural coupling to be exclusively due to bracket fastening (configuration B in Fig. 5c). In order to emulate the free boundary conditions, the system was resting on four air jacks, located close to the corners of the CLT100A1 plate, the internal air pressure of which has been kept constant during the measurements. Each plate was dynamically excited with an inertial shaker emitting

Table 2. Geometrical and mechanical properties of CLT100A1 and CLT060C1 plates. Parameters are referred to the reference system of each plate, in which the z-axis is parallel to the plate thickness and the x-axis is perpendicular to the fibers of the top plies.

Property	Units	Plate ID	
		CLT100A1	CLT060C1
Length	m	2.87	1.52
Width	m	..... 1.14	
Thickness	m	0.10	0.06
Density, ρ	kgm^{-3}	462.00	452.00
Loss Factor, η	-	0.014	0.0083
Elastic Moduli			
E_x	GPa	12.70	11.50
E_y	GPa	0.42	0.38
E_z	GPa	0.42	0.38
Poisson's Ratios			
ν_{xy}	-	..... 0.10	
ν_{yz}	-	..... 0.30	
ν_{xz}	-	..... 0.10	
Shear Moduli			
G_{xy}	GPa	0.79	0.72
G_{yz}	GPa	0.16	0.14
G_{xz}	GPa	0.79	0.72

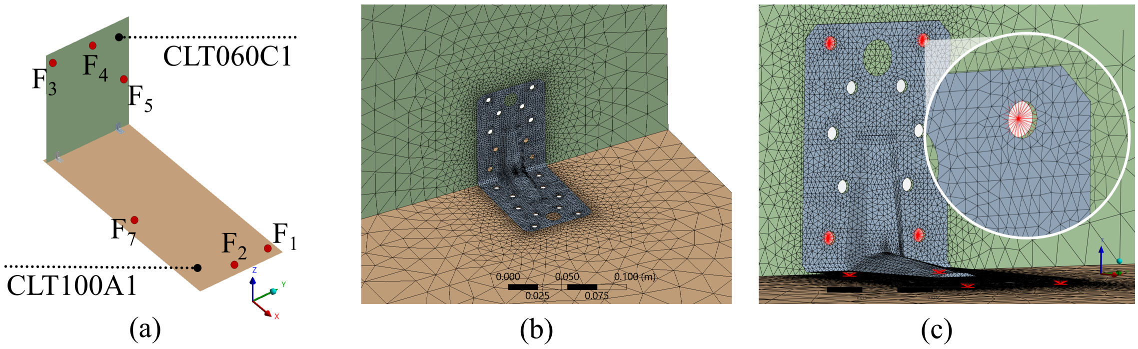

Figure 4. (a) Drawing of the FEM geometry of the L-junction. Excitation points F1 to F7 are highlighted with red dots. (b) Close-up on mesh elements: bracket was modelled with $2\,\mathrm{mm}$ triangular elements. Gradual size transition to the $4\,\mathrm{cm}$ plate mesh was guaranteed. (c) Close-up on the MPC joints defined at the screw positions.

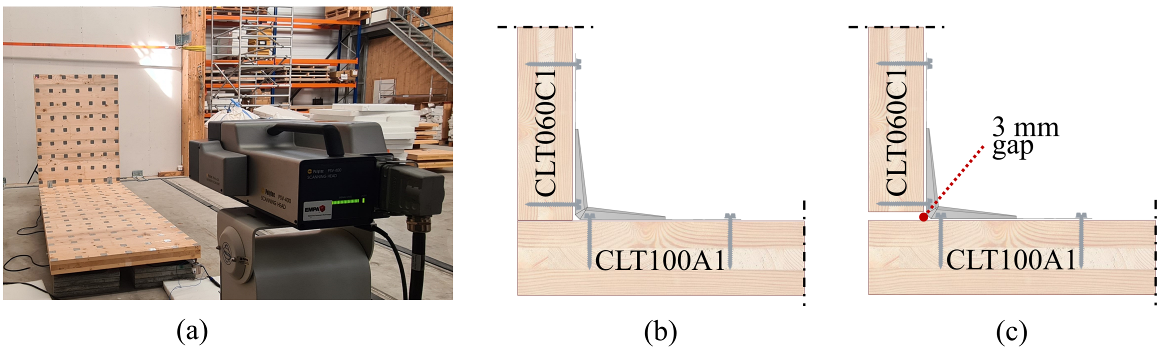

Figure 5. (a) Picture of the CLT L-junction mock-up during the laser doppler vibrometry measurements. (b) Schematization of the configuration A with plates in direct contact. (c) Schematization of the configuration B with a $3\,\mathrm{mm}$ air gap between plates.

a sine sweep signal. For each plate, three different excitation positions were set up, according to the schematization of the numerical model depicted in Fig. 4a. Normal surface velocities were acquired with a Polytec PSV-400 scanning vibrometer pointing normally to the plates, over a 17×7 points regular grid for the CLT100A1 plate, and over a 9×7 points grid for the CLT060C1 plate. Results were exported within the $1\,\mathrm{Hz}$-$5.8\,\mathrm{kHz}$ frequency range with a resolution of $62.5\,\mathrm{mHz}$.

5. RESULTS AND DISCUSSION

5.1 FEM model validation in the modal domain

Results from the FEM modal analysis described in subsection 4.1 were compared for validation to the first fifteen bending and torsional eigenmodes of both experimental configurations, in terms of eigenfrequency PE and MAC. It should be noted that the first rigid-body mode of the junction, occurring below $10\,\mathrm{Hz}$, has not been considered in this analysis. As visible from Fig. 6, a good correlation against both experimental datasets is observable. In particular, PE values were found to be below 10% and, as visible in Fig. 6a, configuration A was stiffer than configuration B, as expected. The minimum MAC value was found to be 0.7 among all modes of both configurations (Fig. 6b,c). This reveals that, in the low-frequency range, edge contact between CLT plates does not significantly affect the modal behaviour of the system. Furthermore, assuming rigid multi-point constraint at screw holes was sufficient to ensure good correlation with experimental data and no further contact modelling is needed at low frequencies.

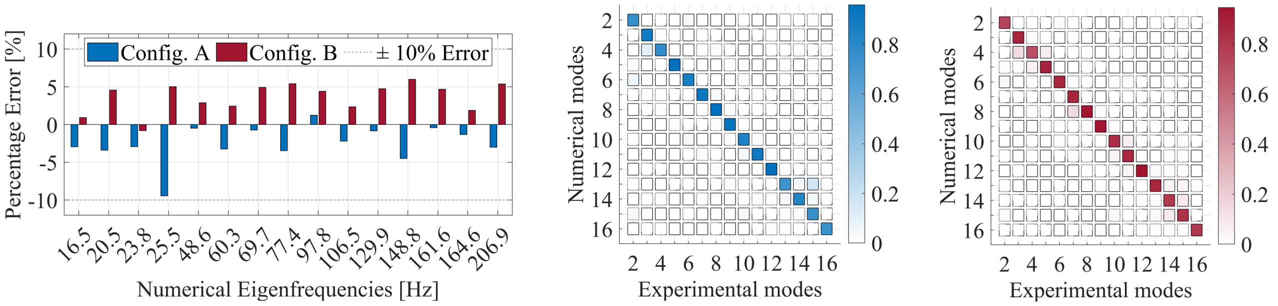

(a) (b) (c)

Figure 6. (a) Percentage error of numerical against experimental eigenfrequencies from configurations A and B. (b,c) Modal Assurance Criterion of numerical against experimental eigenmodes from configuration A (b) and configuration B (c).

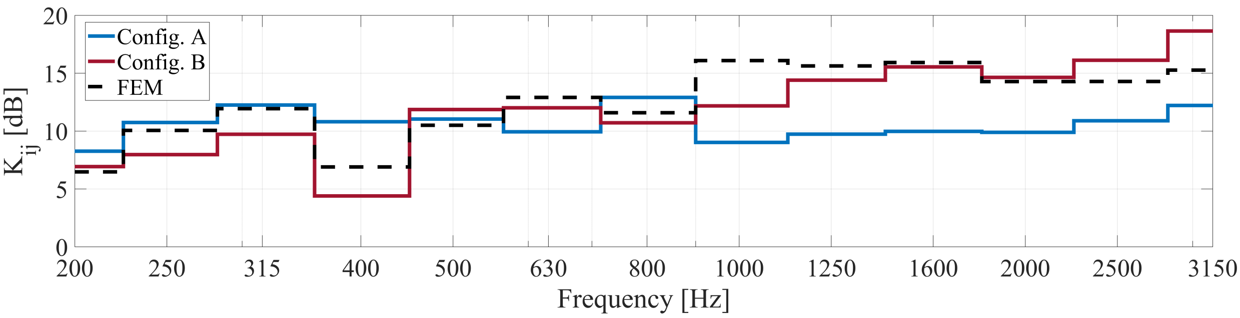

Figure 7. Comparison of numerical and experimental K_{ij} from configurations A and B in one-third octave bands.

5.2 Calculation of the Vibration Reduction Index K_{ij}

As an outcome of the FEM full harmonic analysis, the numerical Vibration Reduction Index K_{ij} was computed and compared to the K_{ij} from configurations A and B in the 200 Hz-3150 Hz frequency range, as shown in Fig. 7. Numerical data show an average deviation of 3.2 dB and a maximum deviation of 7.1 dB at 1 kHz from the experimental K_{ij} of the configuration A, in which the plates were in contact. In addition, the deviation between numerical and experimental single-number K_{ij} was calculated in the mid-frequency (250 Hz - 1 kHz) and high-frequency (1.25 kHz - 3.15 kHz) ranges, as defined in [4]. In the former case, the deviation was equal to 0.5 dB, whilst in the high frequency range it was found to be 4.5 dB. Analysing the overall trend, it appears that the FEM model underestimates the mechanical coupling between the CLT plates above 1 kHz. This can be attributable to possible effects of friction and pre-stress due to the direct contact between the plates in the configuration A, which are neglected in the numerical model. Such effects may be accounted for by introducing non-linear contact conditions or contact stiffness values at the nodes along the common edge between the two plates. These stiffness values may be retrieved from parameter estimation procedures based on curve fitting algorithms against experimental data. As visible in Fig. 7, there is a better agreement between numerical data and K_{ij} from configuration B, in which the plates were separated by an air gap. In particular, the overall trend of numerical K_{ij} is consistent with experimental data over the entire frequency range. An average deviation of 1.7 dB is observed, which almost halves the 3.2 dB mean deviation from the configuration A in the same frequency range. The maximum deviation from configuration B was found to be equal to 3.9 dB at the 1 kHz third octave band. Furthermore, the deviations between numerical and experimental single-number K_{ij} in the mid and high-frequency ranges are respectively equal to 1.6 dB and 0.8 dB. This confirms that the effects of direct contact between plates plays a major role at high frequencies. As a result, it can be stated that the modelling of the bracket with screws can be considered acceptable, although still subject to possible improvements. For example, the use of rigid MPC joints at screw locations could possibly overconstrain the connections at some third octave frequency bands. On this basis, stiffnesses of the screw fastening may be obtained from further experimental investigations and introduced into the model.

6. CONCLUSIONS

This contribution presents a numerical investigation for the prediction of flanking sound transmission across a CLT L-junction, starting from the detailed representation of a commercially available angle bracket. This was modelled in FEM, validated with vibrometry measurements and integrated into a global FEM model of an L-junction mock-up. The numerical K_{ij} was compared with the experimental counterpart from measurements on two different configurations, in which plates were either in contact or separated by an air gap. The analysis provided useful insights on how to model the bracket fastening and the line connections between CLT plates. In particular, the comparison of the numerical K_{ij} with that from the experimental setup in which plates were in direct contact highlighted that the contact forces between plates play a major role and need to be included in numerical models, possibly by means of nodal stiffness values. These can be retrieved from further investigations on experimental data, conceivably with parameter estimation algorithms. A better agreement was observed from the comparison of numerical data against the K_{ij} from the configuration in which plates were separated by a gap. This suggested that modelling the bracket fastening with multi-nodal rigid joints can be partially acceptable, but still subject to possible improvements, e.g. by including nodal stiffnesses along the screw hole edge interfaces in order to reduce coupling overestimation.

7. ACKNOWLEDGMENTS

The presented results were developed within the framework of the cooperative project "Schallschutz im Holzbau" between Lignum and Empa. The project was funded by the Swiss Federal Office for the Environment (FOEN) as part of the Aktionsplan Holz. We gratefully acknowledge this financial support.

8. REFERENCES

[1] L. Cremer and M. Heckl, *Structure-Borne Sound: Structural Vibrations and Sound Radiation at Audio Frequencies*. Berlin, Germany: Springer Science & Business Media, 2013.

[2] F. Morandi, S. De Cesaris, M. Garai, and L. Barbaresi, "Measurement of flanking transmission for the characterisation and classification of cross laminated timber junctions," *Applied Acoustics*, vol. 141, p. 213 – 222, 2018.

[3] International Organization for Standardization, *ISO 12354-1:2017 Building acoustics — Estimation of acoustic performance of buildings from the performance of elements*, 2017.

[4] International Organization for Standardization, *ISO 10848-1:2017 Acoustics — Laboratory and field measurement of flanking transmission for airborne, impact and building service equipment sound between adjoining rooms - Part 1: Frame document*, 2017.

[5] M. Salvalaggio, F. Lorenzoni, and M. R. Valluzzi, "Impact of sound-insulated joints in the dynamic behavior of cross-laminated timber structures," *Journal of Building Engineering*, vol. 91, p. 109525, 2024.

[6] S. Moons, R. Lanoye, and E. P. Reynders, "Prediction of flanking sound transmission through cross laminated timber junctions with resilient interlayers," *Applied Acoustics*, vol. 228, p. 110317, 2025.

[7] S. V. Modak, *Analytical and Experimental Modal Analysis*. Boca Raton, USA: CRC Press Taylor & Francis Group, 2023.

[8] R. Vasile, S. G. Racz, and O. Bologa, "Experimental and numerical investigations of the steel sheets formability with hydroforming," in *Proc. of MATEC Web of Conferences CoSME'16*, p. 02016, 2017.

[9] S. Vallely and S. Schoenwald, "Frequency-independent homogenised elastic and damping constants of cross-laminated timber," in *Proc. of Forum Acusticum 2023*, (Turin, Italy), pp. 1297–1304, 2023.